

# Internal cooling augmentation in rectangular channel using two inclined baffles

Prashanta Dutta<sup>a,\*</sup>, Akram Hossain<sup>b</sup>

<sup>a</sup> *Mechanical and Materials Engineering, Washington State University, P.O. Box 642920, Pullman, WA 99164-2920, USA*

<sup>b</sup> *Civil and Environmental Engineering, Washington State University, Richland, WA 99352-1671, USA*

Received 19 May 2004; accepted 11 August 2004

Available online 7 October 2004

## Abstract

This experimental study investigates the local heat transfer characteristics and the associated frictional head loss in a rectangular channel with inclined solid and perforated baffles. A combination of two baffles of same overall size is used in this experiment. The upstream baffle is attached to the top heated surface, while the position, orientation, and the shape of the other baffle is varied to identify the optimum configuration for enhanced heat transfer. A constant surface heat flux is applied from the top surface, but the bottom and the side surfaces are maintained at an adiabatic condition. The flow Reynolds number for this experimental study is varied between 12,000 and 41,000. The inline placement of baffles augments the overall heat transfer significantly by combining both jet impingement and the boundary layer separation. Experimental results show that the local Nusselt number distribution is strongly depended on the position, orientation, and geometry of the second baffle plate. The friction factor ratio goes up with an increase in the Reynolds number, but its value depends on the arrangement of baffles. Like single inclined baffle and rib-mounted channels, the frictional head loss is much higher for two inclined baffles.

© 2004 Elsevier Inc. All rights reserved.

*Keywords:* Baffle; Heat transfer augmentation; Inclined baffle; Rectangular channel

## 1. Introduction

In modern gas turbines, it has become a growing trend to increase the temperature of the combustion product to increase the specific thrust and to reduce the specific fuel consumption. Such a high temperature is far above the allowable temperature of super alloys and thermal barrier coatings (TBC) used in gas turbine blades. In gas turbine, usually air is used in the interior side of the blade to maintain the blade at the proper working temperature. Also in a number of other engineering and industrial applications such as, air-cooled

solar collectors, laser curtain seals, labyrinth shaft seals, compact heat exchangers, and microelectronics, air is preferred as a coolant for its lightweight. However, due to the very low thermal conductivity internal cooling with gases is less effective than cooling with liquids. There are several techniques available to enhance the heat transfer coefficient of gases in internal cooling. The most commonly used technique for internal cooling enhancement is the placement of periodic ribs. Ribs are generally mounted on the heat transfer surface, which disturbs the boundary layer growth and enhances the heat transfer between the surface and the fluid.

In literature, numerous studies on ribbed channel heat transfer are reported, but only the relevant articles are cited here. Sparrow and Tao (1983) obtained enhanced heat transfer in a rectangular channel by inserting rod-type disturbance elements adjacent to the

\* Corresponding author. Tel.: +1 509 335 7989; fax: +1 509 335 4662.

E-mail address: [dutta@mail.wsu.edu](mailto:dutta@mail.wsu.edu) (P. Dutta).

### Nomenclature

$c_p$	specific heat of air	$q$	amount of heat input
$D$	channel hydraulic diameter	$q_{\text{loss}}$	amount of heat lost to the surroundings
$f$	friction factor	$Re$	Reynolds number based on channel hydraulic diameter
$f_s$	friction factor in smooth pipe at the same Reynolds number	$S_L$	longitudinal pitch of perforated holes
$H$	channel height	$S_T$	transverse pitch of perforated holes
$h$	local heat transfer coefficient at the channel centerline	$T_b$	bulk mean temperature
$k$	thermal conductivity of air	$T_w$	local wall temperature
$L$	length of the baffle	$t$	thickness of the baffle
$M$	number of holes in the longitudinal direction	$U$	channel centerline velocity
$\dot{m}$	mass flow rate of air	$V$	channel mean velocity, $V = 0.766U$
$N$	number of holes in the transverse direction	$W$	width of the baffle
$Nu$	channel centerline Nusselt number	$x$	distance from the start of heating
$Nu_0$	Nusselt number for fully developed pipe flow at the same Reynolds number	<i>Greeks</i>	
$Nu_{\text{av}}$	average Nusselt number at the centerline	$\rho$	density of air
$P$	pressure	$\mu$	viscosity of air

principal wall. In a series of studies, Chandra and co-workers experimentally investigated the heat transfer and associated frictional loss in a rectangular channel with a varying number of ribbed walls (Chandra et al., 1997, 2003). In a separate study, internal cooling heat transfer augmentation is reported for a fully developed turbulent flow in a square channel with V-shaped turbulence promoters (Han et al., 1991). These ribs or surface protuberances are small and do not disturb the core flow. Thus, the turbulence enhancement and boundary layer breakdown are mostly localized near the heat transfer surface, and therefore, the gain in heat transfer coefficient is not significantly offset by the pressure drop penalties.

Another popular heat transfer augmentation technique is impingement cooling that uses high velocity jets to cool the surface of interest. Lin et al. (1997) experimentally showed the heat transfer behavior of a confined single-slot impingement. However, in practical applications often a large region needs to be cooled and multiple jets are required. A multiple jet configuration is normally affected by the cross-flow developed from upstream spent-jets. Goldstein and Seol (1991) have presented the convective heat transfer characteristics from a row of circular air jets formed by the square edged orifices. In a similar experimental work, the effect of excitation on the flow and heat transfer performances is reported (Liu and Sullivan, 1996). Lately, Beitelmal et al. (2000) demonstrated the effect of the impinging jet inclination in cooling a uniformly heated plate. The jet impingement mechanism used in that work is very similar to our current study.

In addition to ribs and impingement, a third common internal cooling enhancement technique is the placement of internal flow swirls, tape twistors, or baffles. The swirl insert and tape twistor techniques create a significant amount of bulk flow disturbance, and the pressure drop penalties are much higher compared to the gain in heat transfer coefficient. Baffles also create bulk flow disturbance, but unlike tapes or swirls, baffles are discrete objects. Therefore, the flow disturbance created by baffles may be localized, but more intense. Usually the baffle plate is attached to the thermally active surface to augment heat transfer by providing additional fin-like surface area for heat transfer and better mixing. In the past, experimental results were published with baffle plates orthogonal to the flow direction (Berner et al., 1984; Habib et al., 1994). Since those works are emphasized on baffles that directly block the flow, the pressure penalties (friction factor) are higher than the heat transfer improvements. However, it is possible to obtain enhanced heat transfer with comparably less frictional head loss by inserting inclined baffles in the flow path. Inclined baffles may be considered as a combination of ribs and channel inserts. These baffles are big enough to disturb the core flow, but like ribs, they are mounted on or near the heat transfer surface. Moreover, inclined perforated baffles contain circular holes, which facilitate jet impingement toward the heat transfer surface. Hence by utilizing inclined perforated baffles, the three major heat transfer augmentation techniques can be combined for effective cooling.

Dutta and Dutta (1998) first reported the enhancement of heat transfer with inclined solid and perforated

baffles. In that study, the effects of baffle size, position, and orientation were studied for internal cooling heat transfer augmentation. Later on, a number of research groups have utilized the perforated baffle concept for internal cooling augmentation both experimentally (Ko and Anand, 2003; Ziolkowska et al., 1999) and numerically (Yang and Hwang, 2003; Yilmaz, 2003; Tsay et al., 2003). In those studies, different aspect ratio channels and different porosity baffles were used. In a recent experimental work, Khan et al. (2002) reported the heat transfer results in a rib mounted baffle channel. However, their pressure penalty was more severe than the inclined baffle results.

In our previous experimental work we have shown that the inclined perforated baffle attached to the heated surface works much better than the corresponding arrangement with solid baffles (Dutta and Dutta, 1998). The inclined perforated baffle allows the jet impingement toward the heated surface to augment the heat transfer. However, in case of single baffle, the region of higher heat transfer is only limited to the baffle mounted zone. While there is little heat transfer improvement downstream of the baffle, the heat transfer characteristics at the upstream of the baffle remain virtually unaltered. In this study, we present experimental heat transfer results with two inclined baffles where the first baffle is mounted on the heated top surface and the second baffle is either fixed to the insulated bottom

surface or to the heated top surface. Depending on the position, orientation and choice of second baffle, we have considered nine different arrangements for this study. The main objective of the present study is to augment both local and global heat transfer behavior of a gaseous fluid (air) by placement of two inclined baffles. Since the flow disturbances and wakes generated by the upstream inclined baffle can potentially affect the performance of the downstream baffle, an average heat transfer performance is considered to cover the entire heated length.

## 2. Experimental apparatus

Fig. 1(a) shows the schematic view (not-to-scale) of the experimental facility that is used in this study. The wind tunnel used for this investigation is made of plexi glass with a cross-section of 24.92 cm × 4.92 cm. Therefore, the aspect ratio for our rectangular channel is approximately 5. We have presented all geometrical dimensions in terms of channel height  $H$  ( $H = 4.92$  cm), while heat transfer coefficients and friction factors are presented in terms of channel hydraulic diameter,  $D$  ( $D = 8.217$  cm). A suction-mode blower is used to draw air through a contraction followed by flow straighteners and the rectangular wind tunnel. The flow develops through a  $31H$  long unheated entrance before

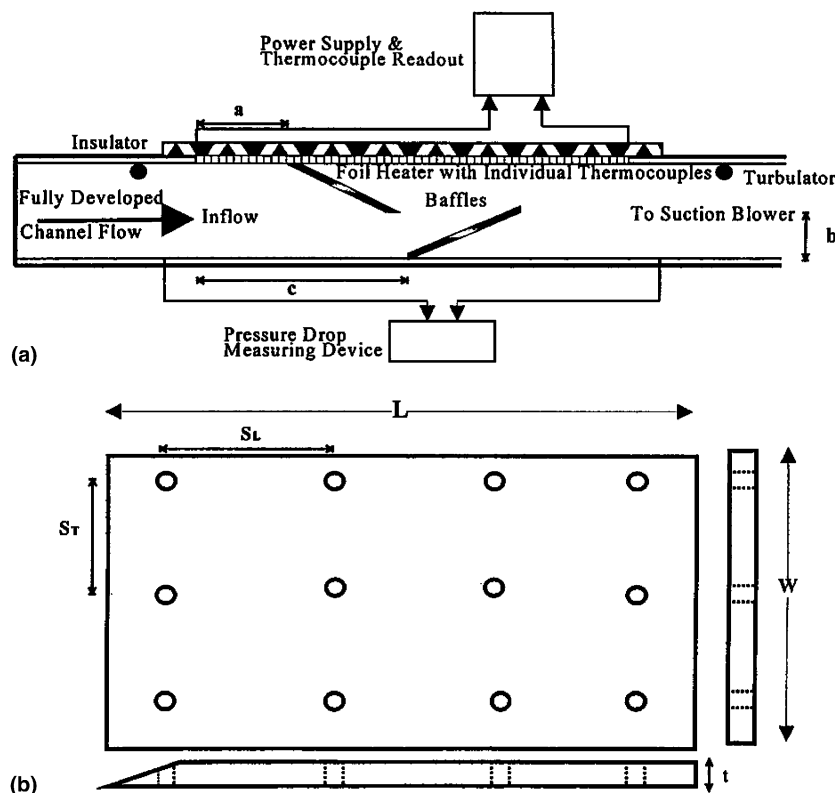


Fig. 1. (a) Schematic diagram of the experimental setup; (b) a perforated baffle plate with associated nomenclature.

entering the heated test section. The heated test section is  $19.2H$  long, and the exit of the wind tunnel is at a  $22.2H$  distance downstream of the heated test section.

Uniform heat flux heaters are fabricated from stainless steel foils. A total of 46 iso-flux heaters of identical size are mounted on the upper surface of the test section, and they are aligned perpendicular to the flow direction. These heaters are connected in series with an online voltage controller in order to supply the same amount of heat to each heater. All other sides of the channel are unheated. Commercial fiberglass insulation is used on the external surfaces to prevent any thermal energy leakage due to convection and radiation. For wall temperature measurement, heaters are connected to copper-constantine thermocouple glued at the center of the foil heater. Moreover, one thermocouple is placed at the inlet ( $1.55H$  upstream of the heated test section) and two others are positioned at the outlet ( $2.3H$  downstream of the heated test section) to measure the inlet and outlet bulk fluid temperatures, respectively. Each thermocouple is calibrated against a standard thermal bath over the range of the operating temperatures. Two wooden turbulators are attached to the top wall at  $1.55H$  upstream and  $2.3H$  downstream of the heated test section. These turbulators are placed to ensure a turbulent boundary layer and good mixing of the bulk flow for mean temperature measurement. Two pressure probes are used to measure the frictional head loss, and they are located at  $2.45H$  upstream and  $4.4H$  downstream of the heated test section.

In this study, both solid and perforated baffles of same overall size (length,  $L = 29$  cm; width,  $W = 24.92$  cm; and thickness,  $t = 5$  mm) are utilized. The schematic view of a perforated baffle used in this investigation is given in Fig. 1(b). The leading edges of the baffle plates are kept sharp to reduce the flow disturbance by the protruding edge. Perforations are created by drilling holes through the baffle plate. All perforated baffles have uniform holes of diameters,  $d = 1.07$  cm. A total of three baffles, two perforated and one solid, is used in this experiment, and the summary of these plexi glass baffles is presented in Table 1.

Table 2 shows the different configuration investigated in this study. In all configurations, baffle #1 is used as a first plate, and it is placed at a distance of  $1.25$  cm ( $a = 0.25H$ ) downstream from the start of the first foil heater. Either of the remaining two baffles (baffle #2

Table 1  
Identification of baffles used in this study

Baffle #	Type	Length $L$ (cm)	Longitudinal pitch ( $S_L$ ) (cm)	Transverse pitch ( $S_T$ ) (cm)	$M$	$N$
1 and 2	Perforated	29	6.35	6.04	4	3
3	Solid	29	No holes	No holes	0	0

Table 2  
Different baffle configurations used in these internal cooling experiments

Configuration	$c$ (cm)	Baffle # for second plate	Attachment of second plate
A	29.20	2 (perforated)	Top surface
B	29.20	2 (perforated)	Bottom surface
C	44.45	2 (perforated)	Top surface
D	44.45	2 (perforated)	Bottom surface
E	60.02	2 (perforated)	Top surface
F	60.02	2 (perforated)	Bottom surface
G	29.20	3 (solid)	Bottom surface
H	44.45	3 (solid)	Bottom surface
I	60.02	3 (solid)	Bottom surface

In all cases, the baffle #1 is attached to the heated top surface ( $a = 1.25$  cm and  $b = 2.54$  cm). A 3 mm allowance is provided between heaters and the baffle if the baffle is oriented with the top surface of the channel.

and #3) is attached to the heated top surface or to the insulated bottom surface. If a baffle is attached to the heated top surface, a 3 mm gap is maintained between heated top surface and the baffle to prevent possible burn out of the heater at the baffle contact. In all arrangements, a constant inclination angle of five degrees is maintained for both plates. This small inclination angle keeps these plates streamlined with the flow, and hence they avoid major flow blockage. Depending on the selection of baffle #2 or #3 and their relative positions, nine different arrangements (A to I) were studied as shown in Fig. 2(a–c).

### 3. Theory

The local heat transfer coefficient,  $h$ , is obtained as

$$h = \frac{q - q_1}{A_s(T_w - T_b)} \quad (1)$$

where,  $A_s$  is the surface area of the heater,  $T_w$  is the wall temperature, and  $T_b$  is the bulk mean temperature. The heat input,  $q$ , from the heaters are calculated as

$$q = VI \quad (2)$$

where  $V$  and  $I$  are the voltage and current applied across the heaters, respectively. The heat lost,  $q_1$ , is estimated from a separate heat loss experiment done on the test facility without airflow. A heat loss characteristic curve is developed for each thermocouple location and it is found that the maximum local heat loss,  $q_1$ , is less than 5% of the total local heat supplied,  $q$ . The wall temperature is measured directly by the thermocouple attached to foil heater and the bulk temperature is calculated from the energy balance, i.e., bulk temperature increase is equal to the net thermal energy supplied to the air stream divided by the mass flow rate,  $\dot{m}$ , and specific heat,  $c_p$ . In this study, the wall to ambient temperature difference is kept below  $35^\circ\text{C}$  and the bulk temperature

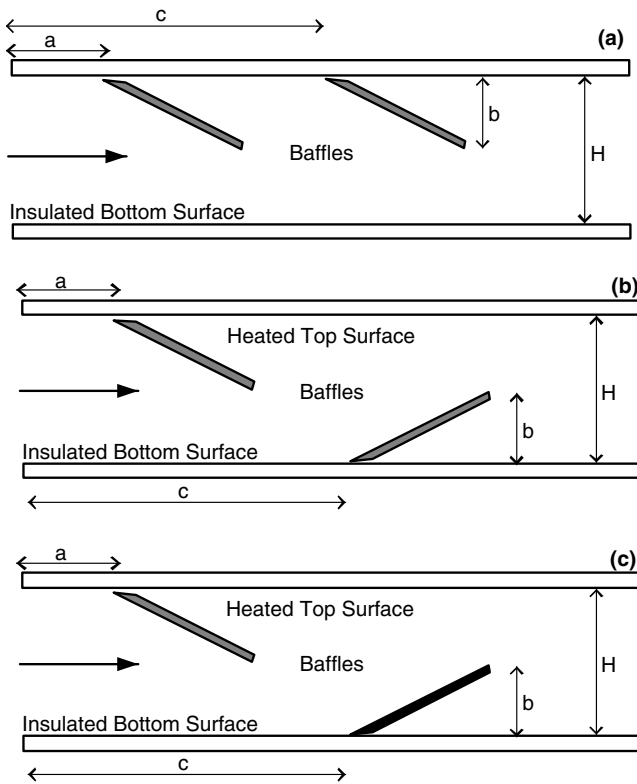


Fig. 2. Relative positions of baffles in the test section: (a) for configurations A, C, and E; (b) for configurations B, D, and F; (c) for configurations G, H, and I.

rise from inlet to outlet is less than 3°C. The flow Reynolds number is calculated as

$$Re = \frac{\rho VD}{\mu} \quad (3)$$

where  $\rho$  is the fluid density,  $\mu$  is the fluid viscosity,  $V$  is the channel average velocity and  $D$  is the channel hydraulic diameter. Although the channel centerline velocity is measured using a pitot-static tube, a relation is derived to get an average velocity,  $V$ , from centerline velocity,  $U$ , ( $V = 0.766U$ ) for turbulent flow by using  $1/7^{\text{th}}$  power law. The mass flow rate within the channel is varied by changing the flow area of the suction blower, and the flow Reynolds number in this study is ranged between 12,000 and 41,000. Since all experimental results are presented for air at a single characteristics dimension ( $D = 8.217\text{cm}$ ), the flow Reynolds number range presented in this study corresponds to the lower and upper pumping capabilities of the suction blower. The local Nusselt number is calculated as

$$Nu = \frac{hD}{k} \quad (4)$$

where  $k$  is the thermal conductivity of the fluid. The average Nusselt number,  $Nu_{av}$ , is the arithmetic average of all local Nusselt numbers along the heated part of the

channel. The friction factor is evaluated from the pressure drop as

$$f = \frac{\Delta PD}{\frac{1}{2}L_e\rho V^2} \quad (5)$$

where  $\Delta P$  is the pressure drop across the heated test section and  $L_e$  is the length of the heated test section. A micromanometer is used to find the pressure drop along the channel with and without baffles. Since two pressure taps are located upstream and downstream of the actual test section, a correction on the pressure drop is performed based on the smooth channel analysis. The extra lengths (probe locations are  $2.45H$  upstream and  $4.4H$  downstream) are assumed to have smooth channel pressure drop properties, and this pressure drop is deducted from the measured pressure drop to get the pressure penalty in the test section. In this study, the pressure drop correction is less than 4% of the total pressure drop.

### 3.1. Uncertainty estimation

A detailed uncertainty analysis is performed for this experimental study. The overall uncertainty of the experimentally measured variables are calculated as (Coleman and Steele, 1998)

$$U_i = \sqrt{B_i^2 + P_i^2} \quad (6)$$

where  $B_i$  is the systematic or bias error and  $P_i$  is the precision or random error of measured variable  $i$ . The variables measured in this experiment are wall temperature, pressure drop, voltage and current of the power source. In our experiment, the bias error is very small compared to the precision error. The error propagation equation developed by Kline and McClintock (1953), is used to calculate the uncertainty of Nusselt number, Reynolds number and friction factor. The maximum uncertainty in calculating the flow Reynolds number is estimated to be  $\pm 4\%$ . Uncertainties of the measured heat flux and calculated Nusselt numbers are within  $\pm 2.5\%$  and  $\pm 5\%$ , respectively. On the other hand, the maximum possible error in the calculated friction factor is  $\pm 7\%$ .

## 4. Results and discussion

The heat transfer coefficient calculations are done on the heated top surface, while the bottom and side surfaces are unheated. All heat transfer results are presented in terms of a non-dimensional Nusselt number ratio ( $Nu/Nu_0$ ) along the channel centerline.  $Nu_0$  is the Nusselt number for fully developed flow in a smooth pipe at the same Reynolds number, and is given by

$$Nu_0 = 0.023Re^{0.8}Pr^{0.4} \quad (7)$$

The  $Nu_0$  is used as a reference to minimize the Reynolds number effect in the presented results. The Nusselt number ratio essentially indicates the amount of enhancement in heat transfer obtained by the flow disturbance promoters over the smooth circular pipe. The experimental procedure is validated by running an experiment through the rectangular setup without any baffle. For this smooth rectangular channel, the thermally fully developed flow is achieved at  $x = 5.0H$  downstream from the start of heating, and the fully developed Nusselt number ratio is found between 1.41 and 1.53. There are two reasons for higher than unity Nusselt number ratio: First, the centerline surface temperature is used in the heat transfer coefficients calculation instead of the span averaged values, and second, in higher aspect ratio channels the Nusselt number is expected to be greater than that for a circular pipe (Kays and Crawford, 1980). For experimental results with inclined baffle(s) three different Reynolds numbers are considered for each arrangement to demonstrate the effects of flow velocity on the heat transfer. Since the reference Nusselt number,  $Nu_0$ , is based on the fully developed flow, we expect to have some Reynolds number dependency in the flow path due to the jet impingements, reattachment, and recirculation.

Fig. 3(a) and (b) illustrate the centerline Nusselt number distribution for configurations A and B, respectively. In configuration A, the second plate is attached to the heated top surface and in configuration B, the second plate is mounted on the insulated bottom surface. In both cases, baffle #2 is used as the second baffle, and the location of the second plate ( $c = 29.20\text{cm}$ ) is exactly the same. However, the orientation of second plate in configuration B is the mirror image of configuration A. As expected, the local Nusselt number ratio is quite high at the start of the heating section due to the development of the thermal boundary layer. From a separate experiment, it has been found that at the thermal entry region, the local Nusselt ratio varies from 2.94 to 3.58 for this smooth rectangular channel. The placement of the first baffle at the beginning of the heated section ( $a = 1.25\text{cm}$ ) disturbs the boundary layer formation and contributes to higher heat transfer. These local peaks are certainly due to the jet impingement from the lower confined section. Here multiple impinging jets develop cross flow and enhance the heat transfer coefficient. The magnitude of the heat transfer enhancement remains almost the same as it was for single perforated baffle attached to the heated top surface at a distance  $a = 1.25\text{cm}$  from the beginning of the heated section (Dutta and Dutta, 1998).

Like single baffle study, sharp decreasing trend is observed at the end of first baffle and the heat transfer coefficient falls below normal ( $Nu/Nu_0 < 1.4$ ) at that region ( $x/H = 5.0$ ) due to the divergent chamber and flow recirculation. However, for configurations A and B, the

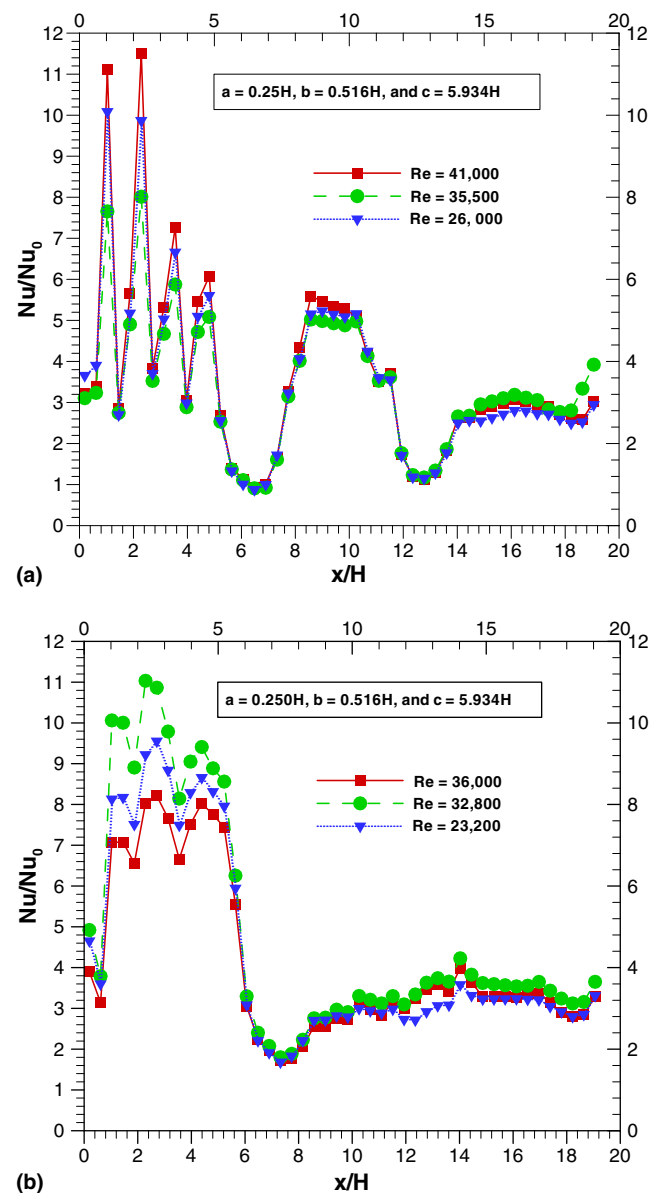


Fig. 3. Local Nusselt number distribution along the channel at different Reynolds number: (a) configuration A; (b) configuration B.

flow patterns are further disturbed due to the presence of the second baffle immediately after the first baffle. Since in configuration A (see Fig. 3(a)), the orientation of the second baffle is exactly same as the first one, an identical Nusselt number distribution is observed at the place of second baffle. But the magnitude of Nusselt number ratio is slightly less at the place of second baffle than its corresponding value observed in the first baffle. This is due to the relatively weaker flow strength at the upstream of the second baffle resulted from the disturbances of the first baffle. In configuration B (see Fig. 3(b)), a different heat transfer pattern is obtained for the second plate. No impingement action is noted here for the second plate, but the flow is streamlined and pushed towards the heated surface with an overall good

cooling. Here the second plate creates another converging conduit. Hence the flow velocity and the corresponding Nusselt number increase from  $x/H = 7.0$  until it reaches a peak at  $x/H = 14$ . Though the converging channel formed by the second plate ends at  $x/H = 12$ , the flow acceleration will continue until  $x/H = 14$  due to the inertia effect.

The heat transfer characteristics distribution for configurations C, D, E and F are presented in Figs. 4 and 5. As in configurations A and B, baffle #2 is used as the second plate for all four configurations (C, D, E and F). In configurations C and D, the second baffle is mounted 44.45 cm away from the beginning of the first heater, while for configurations E and F the second plate

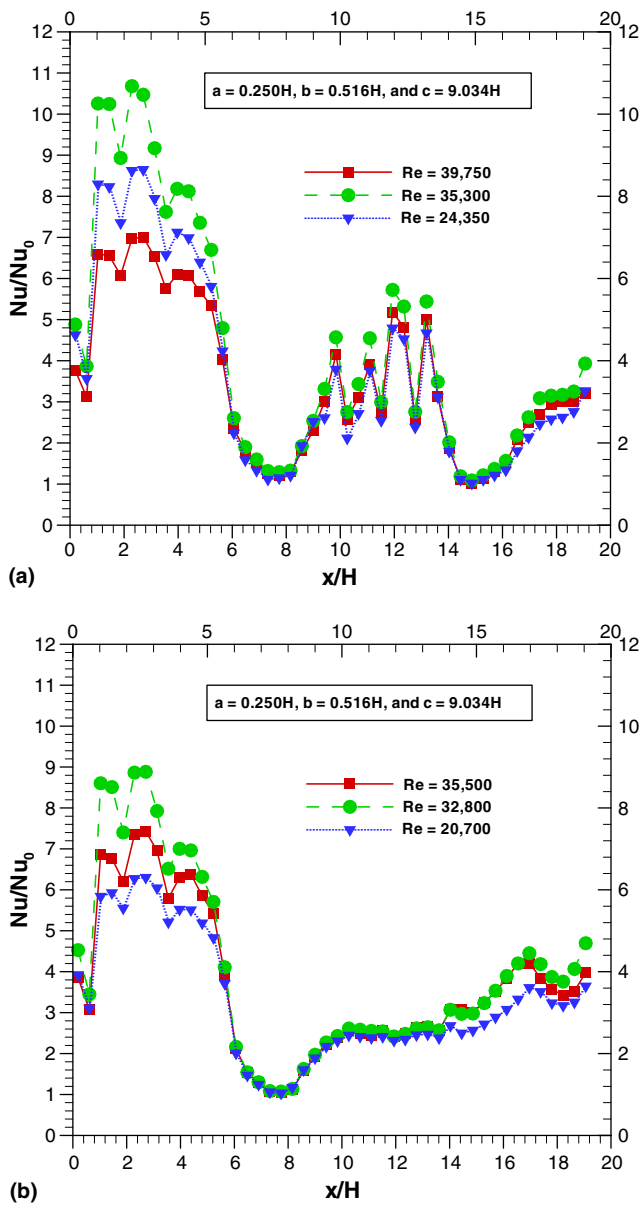


Fig. 4. Local Nusselt number distribution along the channel at different Reynolds number: (a) configuration C; (b) configuration D.

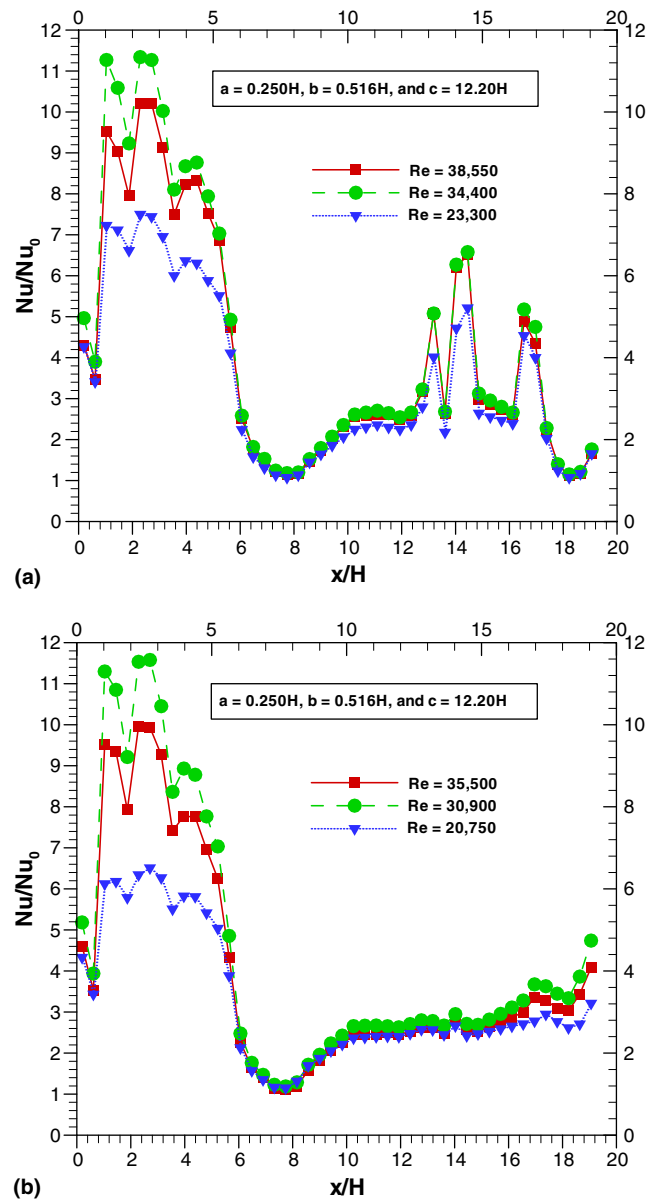


Fig. 5. Local Nusselt number distribution along the channel at different Reynolds number: (a) configuration E; (b) configuration F.

is fixed at  $c = 60.02$  cm. The orientation of the second plate in configurations C and E is similar to orientation of second baffle in arrangement A. Therefore, the heat transfer behavior in Fig. 4(a) and Fig. 5(a) is similar to Fig. 3(a), except a few differences in the region between first and second baffles. From Fig. 4(a) and Fig. 5(a), it is evident that the secondary peaks shift with the second baffle. Also jet impingement strength becomes stronger as the location of the second plate is moved further downstream of the channel. This is due to the fact that as the distance between first and second plate increases, the bulk flow disturbances caused by the upstream baffle relax, and the jet impingements become stronger as the flow passes through the converging

section of the second baffle. The initial higher value of local Nusselt number ratio ( $Nu/Nu_0$ ) before the second baffle in arrangement E (see Fig. 5(a)) can be attributed to the flow reattachment from the first baffle. Arrangement E offers better heat transfer improvement than arrangements A and C by allowing stronger jet impingement on second plate as well as by providing an interim reattachment zone between the first and second baffle. However, in configuration E the second reattachment zone after the second baffle is outside the heating region. The heat transfer trends from Figs. 3(a) and 4(a) show that configuration E can effectively cool longer heating length in the downstream direction.

In configurations D and F, the orientation of the second plate is similar to the orientation of second baffle used in the arrangement B. Hence, Figs. 4(b) and 5(b) follow almost identical heat transfer characteristics of arrangement B where the second plate is mounted with the insulated bottom surface. As the distance between first and second baffles increases (configurations D and F), the flow from the first baffle starts recirculating on the heated top surface. This recirculation contributes to the lower heat transfer coefficient at the end of the first baffle for configurations D and F. Since in arrangement B, the second plate starts immediately after the first baffle, the recirculating zone is very short for this configuration (see Fig. 3(b)). This is due to the fact that in configuration B, the flow convergence provided by the second plate offers resistance to the recirculating fluid. Therefore, arrangement B is preferable to arrangement D or F in deflecting the bulk flow toward the heated surface.

Fig. 6 presents the local Nusselt number ratio distribution at the centerline of the channel for arrange-

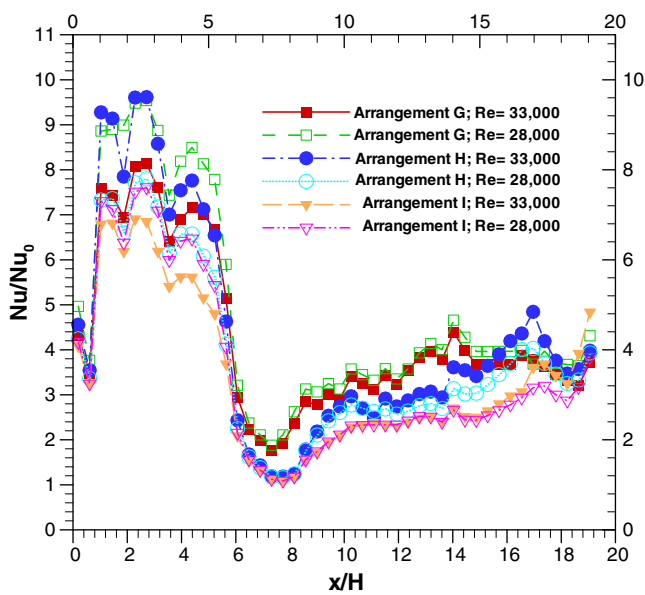


Fig. 6. Local Nusselt number distribution along the channel at different Reynolds number for configurations G, H, and I.

ments G, H, and I. The overall configuration of arrangements G, H, and I are similar to arrangements B, D, and F, respectively. However, for configurations G, H, and I, the second plate is solid instead of perforated. Here the second (solid) plate does not allow any flow leakage and it deflects the entire flow toward the heated top surface. Like configuration B, arrangement G allows smaller recirculation zone than arrangement H or I. Moreover, in configuration G, the fluid faces the convergent section early, and hence the velocity of fluid starts increasing from the trailing edge of the first baffle. This contributes to higher heat transfer coefficient in arrangement G than that of arrangement H or I. From Fig. 6, it is clear that heat transfer augmentation starts from the second plate and it continues far downstream of the second plate. Although configuration G is better for the case presented here, configuration I would be effective for cooling a longer heated section. For arrangements G, H, and I, the impingement effect in the first baffle is not as prominent as it was for arrangements B, D, and F. It can be argued that the solid plate (second baffle) in arrangements G, H, and I, offers more resistance (back pressure), and therefore, less air can pass through the holes of the first baffle.

The amount of improvement achieved by two baffles over a single baffle is shown in Fig. 7 for Reynolds number,  $Re = 33,000$ . For single baffle experiments, we have placed the baffle close to the heated top surface. In this case, the baffle was aligned to the flow direction with a  $5^\circ$  angle, and the baffle was positioned at  $6H$  from the beginning of the first strip heater. Also for single baffle case, only perforated (baffle #1) baffle was used to iden-

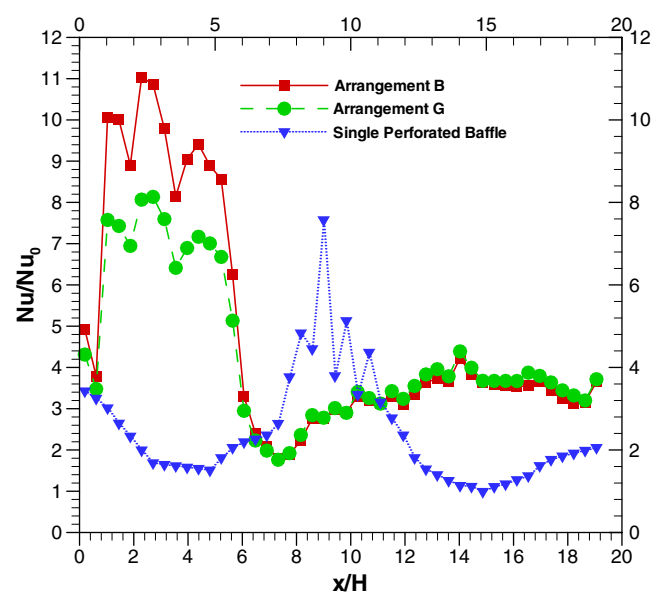


Fig. 7. Comparison of local Nusselt number along the channel centerline for one baffle and two baffles at  $Re = 33,000$ .

tify the heat transfer characteristics, since the heat transfer results for perforated baffles are much better than that of solid baffle. On the other hand, heat transfer results for configurations B and G are plotted for two baffle cases. It is found that a single baffle enhances the heat transfer locally, but for effective cooling of a longer region, placement of two baffles is better. From Fig. 7, it is also evident that two baffles is better than single plate not only for local, but also for average heat transfer enhancement. An optimum combination of two or more baffles will provide higher heat transfer characteristics for a longer cooling zone.

Fig. 8 shows the friction factor ratio,  $ff_0$ , for configurations B, D, F, G, H, and I. Here  $f_0$  is the friction factor in a fully developed smooth pipe at the same Reynolds number, and it can be presented as

$$f_0 = \frac{1}{(0.790 \ln Re - 1.64)^2} \quad (8)$$

The friction factor ratio indicates the penalty in pumping power due to baffles. The two sided ribbed channel results of Chandra et al. (2003) are also plotted for comparison. Note that the aspect ratio of the present work is 2.5 times greater than the ribbed channel used by Chandra and co-workers. Kays and Crawford (1980) reported that for a fully developed flow, the friction factor increases with the aspect ratio. Therefore, the friction factors in the present channel for smooth case is almost 1.25 times higher than the channel of aspect ratio (2:1) used in Chandra et al. (2003). Fig. 8 shows that the arrangement B, D, and F have lower friction factors than those of G, H, and I. This is because of the fact that

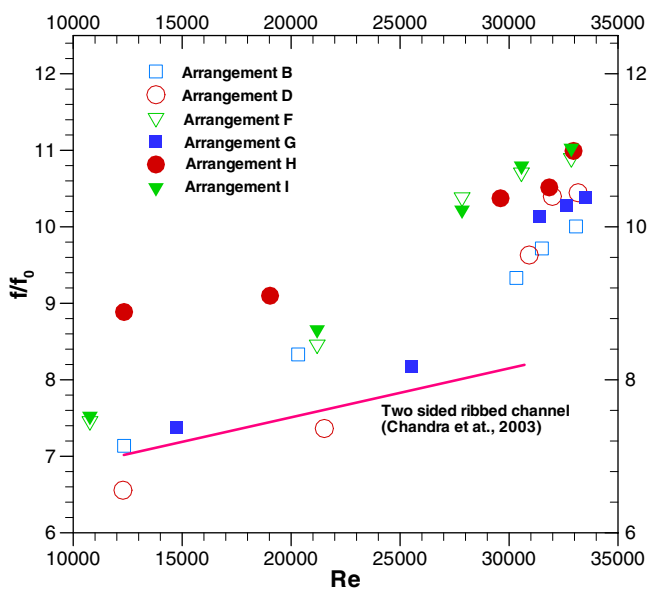


Fig. 8. Variation of friction factor with flow Reynolds number for configurations B, D, F, G, H, and I.

in latter arrangements solid plate is used as the second baffle instead of the perforated one. At higher Reynolds numbers, the frictional loss is mostly higher than the two-sided ribbed channel. Like the ribbed channel results of Chandra et al. (2003), an increase in friction factor ratio is noted with an increase in the flow Reynolds number.

The average heat transfer performance obtained from the whole heated section is presented in Table 3. This table also indicates the relative merit of using baffles based on pumping loss occurred in the flow path. Since perforated baffle arrangements provide less frictional head loss, arrangements A through F are listed in this table. Table 3 indicates that the friction factor can significantly vary with the arrangements of the baffles, but the average Nusselt number ratio stays between 3.26 and 4.82. In order to compare the improvement obtained from two baffles, single baffle results are also presented. Experimental results show that the average Nusselt number ratio is much higher with two baffles than that with a single baffle, but the friction factor ratio can be lower or higher than the single baffle results. It can be argued that the heat transfer in a two-baffle case is high due to more jet impingements, while friction factor is comparable (in some cases) with the single baffle due to a weaker reattachment region downstream of the first baffle.

Table 3  
Overall heat transfer performance improvements and related frictional pressure drops for different configurations

Configuration	Re	$Nu_{av}/Nu_0$	$ff_0$
A	35,500	3.369	5.242
	26,000	3.458	4.414
	41,000	3.637	5.833
B	36,000	4.115	10.231
	23,200	4.299	6.869
	32,800	4.800	9.732
C	39,750	3.495	5.739
	24,350	3.690	5.342
	35,300	4.347	5.634
D	20,700	3.276	7.024
	35,500	3.649	8.725
	32,800	3.985	10.412
E	23,300	3.449	4.850
	38,550	4.152	6.918
	34,400	4.441	6.263
F	20,750	3.261	8.028
	35,500	3.979	11.121
	30,900	4.456	10.722
Single baffle	24,750	2.013	5.228
	35,500	2.211	5.556
	29,200	2.403	5.397

In case of single baffle experiments, baffle #1 is attached to the heated top surface (with a 3 mm gap) and is aligned to the flow direction at a 5° angle.

## 5. Conclusions

This paper presents experimental results for heat transfer in a rectangular channel with two inclined baffles. A constant heat flux is applied from the top surface of the channel, while other surfaces are maintained at adiabatic condition. The flow Reynolds number is varied between 12,000 and 41,000, and the baffle locations and orientations are varied to obtain a wide range of results. The heat transfer and friction factor results are presented in non-dimensional ratios to minimize the Reynolds number dependency. Main conclusions emerging from this study are as follows:

- The local Nusselt number ratio with two inclined baffles significantly depends on the arrangement (orientation, perforation, and position of the baffles) used. Two inclined baffles augment the local heat transfer coefficient for a longer region of interest.
- The overall heat transfer coefficient is much higher with two inclined baffles than that with a single baffle placed in the same channel. The average Nusselt number can be as high as 5.0 times the average Nusselt number of a smooth channel.
- Localized high heat flux zones can be effectively cooled with properly designed perforated baffles in those regions.
- The local Nusselt number ratio is not a strong function of flow Reynolds number. However, in a particular arrangement the friction factor ratio increases with increase in the flow Reynolds number.
- For two inclined baffle cases, the frictional head loss is much higher than that of a single baffle arrangement. Moreover, in two baffle cases the friction factor ratio is larger if the second baffle is attached to the bottom plate instead of the top heated surface.

## References

- Beitelmal, A.H., Saad, M.A., Patel, C.D., 2000. The effect of inclination on the heat transfer between a flat surface and an impinging two-dimensional air jet. *Int. J. Heat Fluid Flow* 21 (2), 156–163.
- Berner, C., Durst, F., McEligot, D.M., 1984. Flow around baffles. *ASME J. Heat Transfer* 106, 743–749.
- Chandra, P.R., Niland, M.E., Han, J.C., 1997. Turbulent flow heat transfer and friction in a rectangular channel with varying number of ribbed walls. *J. Turbomach.* 119 (2), 374–380.
- Chandra, P.R., Alexander, C.R., Han, J.C., 2003. Heat transfer and friction behaviors in rectangular channels with varying number of ribbed walls. *Int. J. Heat Mass Transfer* 46 (3), 481–495.
- Coleman, H.W., Steele, W.G., 1998. *Experimentation and Uncertainty Analysis for Engineers*. John Wiley and Sons Inc., New York.
- Dutta, P., Dutta, S., 1998. Effect of baffle size, perforation and orientation on internal heat transfer enhancement. *Int. J. Heat Mass Transfer* 41 (19), 3005–3013.
- Goldstein, R.J., Seol, W.S., 1991. Heat transfer to a row of impinging circular air-jets including the effect of entrainment. *Int. J. Heat Mass Transfer* 34 (8), 2133–2147.
- Habib, M.A., Mobarak, A.M., Sallak, M.A., Abdel Hadi, E.A., Affify, R.I., 1994. Experimental investigation of heat transfer and flow over baffles of different heights. *ASME J. Heat Transfer* 116 (2), 363–368.
- Han, J.C., Zhang, Y.M., Lee, C.P., 1991. Augmented heat transfer in square channels with parallel, crossed and v-shaped angled ribs. *ASME J. Heat Transfer* 113 (3), 590–596.
- Kays, W.M., Crawford, M.E., 1980. *Convective Heat and Mass Transfer*. McGraw Hill, New York.
- Khan, J.A., Hinton, J., Baxter, S.C., 2002. Enhancement of heat transfer with inclined baffles and ribs combined. *J. Enhanced Heat Transfer* 9 (3–4), 137–151.
- Kline, S.J., McClintock, F.A., 1953. Describing uncertainties in single-sample experiments. *Mech. Eng.*, 3–8.
- Ko, K.H., Anand, N.K., 2003. Use of porous baffles to enhance heat transfer in a rectangular channel. *Int. J. Heat Mass Transfer* 46 (22), 4191–4199.
- Lin, Z.H., Chou, Y.J., Hung, Y.H., 1997. Heat transfer behaviors of a confined slot jet impingement. *Int. J. Heat Mass Transfer* 40 (5), 1095–1107.
- Liu, T.S., Sullivan, J.P., 1996. Heat transfer and flow structures in an excited circular impinging jet. *Int. J. Heat Mass Transfer* 39 (17), 3695–3706.
- Sparrow, E.M., Tao, W.Q., 1983. Enhanced heat transfer in a flat rectangular duct with streamwise-periodic disturbances at one principal wall. *ASME J. Heat Transfer* 105, 851–861.
- Tsay, Y.L., Cheng, J.C., Chang, T.S., 2003. Enhancement of heat transfer from surface-mounted block heat sources in a duct with baffles. *Numer. Heat Transfer Part A* 43 (8), 827–841.
- Yang, Y.T., Hwang, C.Z., 2003. Calculation of turbulent flow and heat transfer in a porous-baffled channel. *Int. J. Heat Mass Transfer* 46 (5), 771–780.
- Yilmaz, M., 2003. The effect of inlet flow baffles on heat transfer. *Int. Commun. Heat Mass Transfer* 30 (8), 1169–1178.
- Ziolkowska, I., Dolata, M., Ziolkowski, D., 1999. Heat and momentum transfer in fluids heated in tubes with turbulence generators at moderate Prandtl and Reynolds numbers. *Int. J. Heat Mass Transfer* 42 (4), 613–627.